Digital Filtering, Calibration and Correlation Analysis of Radar-Echoes from the Tropo- and Stratosphere

by

R. Rüster and R.F. Woodman

Max-Planck-Institut für Aeronomie, D-3411 Katlenburg-Lindau 3

Abstract:

VHF-radars have been successfully used for remote sensing of the lower and middle atmosphere. The received radar-echoes are digitized and these raw data are processed in several sequential steps. By digitally filtering the raw data which is equivalent to a compression or a coherent integration, the amount of data is reduced and at the same time the signal-to-noise ratio is increased. After this pre-integration procedure the compressed data are calibrated and digitally corrected. Using correlation methods the spatial and temporal variations of the echo-power as well as the velocity of the reflecting or backscattering medium are determined. Results of measurements using the Jicamarca radar facility and the SOUSY-VHF-radar are presented.

Zusammenfassung:

VHF-Radarsysteme sind erfolgreich zur Untersuchung der unteren und mittleren Atmosphäre eingesetzt worden. Die empfangenen Radarechos werden digitalisiert und diese Rohdaten in verschiedenen Schritten verarbeitet. Durch digitale Filterung der Rohdaten, die einer Kompression oder einer kohärenten Integration entspricht, wird die Datenmenge reduziert und gleichzeitig das Signal/Rausch-Verhältnis verbessert. Im Anschluß an diese Vorintegration werden die komprimierten Daten digital korrigiert. Mit Hilfe von Korrelationsmethoden lassen sich die räumlichen und zeitlichen Variationen der Echo-Intensität sowie der Geschwindigkeit des reflektierenden oder rückstreuenden Mediums bestimmen. Ergebnisse, die mit der Jicamarca-Radaranlage und dem SOUSY-VHF-Radar gewonnen wurden, werden diskutiert.

1. Introduction

In the last few years VHF-Doppler-Radars have proved to be powerful tools for investigating the structure and the dynamics of the lower and middle atmosphere (Crane (1970), Woodman and Guillen (1974), Cunnold (1975), Green et al. (1975), Rastogi and Bowhill (1975), VanZandt et al. (1975), Aso et al. (1977), and Balsley et al. (1977)). The SOUSY-VHF-radar (Czechowsky et al., 1975) operates at 53.5 MHz in its first phase of development. In the design of this facility measurements have been carried out in 1975 using the 50 MHz-radar at Jicamarca/Peru (Rüster and Woodman, 1976).

It is the purpose of this paper to report the mathematical methods and results of the data-processing, starting from the input signal up to physical quantities as derived from examples obtained by the SOUSY- and Jicamarca-radar.

2. Data-processing of radar signals from the lower and middle atmosphere

One of the most important quantities in measuring dynamical processes with a radar is the pulse period Δt_p. It has to be chosen such that it is much smaller than the characteristic time of the physical processes of interest. First measurements made by Woodman and Guillen (1974) show that this characteristic time is of the order of several seconds in the lower and middle atmosphere.

Since, however, short period statistical variations are superimposed on the signals, Δt_p has to be chosen smaller than the characteristic time by a factor of about 1000. If signals from 300 different heights are recorded the incoming data-rate becomes about one mega-word per second. The processing of such a high data-rate needs special treatment which will be described below.

2.1 Digital Filtering

Because of the high data-rate a data reduction has to be applied before any further processing.

The signal $\underline{s}$ scattered at a height h_i and received at a time t_j carries two items of information (i.e. amplitude and phase, or real and imaginary part). We will use the following nomenclature

$$\underline{s}(h_i, t_j) = \begin{pmatrix} s_R(h_i, t_j) \\ s_I(h_i, t_j) \end{pmatrix} \tag{1}$$

For estimating the characteristic time scales of the observed signals the autocorrelation functions

$$\underline{C}(h_i, \tau) = \frac{1}{N} \sum_{j=1}^{N} \underline{s}(h_i, t_j) \cdot \underline{s}^*(h_i, t_j + \tau) \tag{2}$$

for the various heights are calculated.

The correlation time τ_ε of the intensity of the received signal corresponds to the time interval within which the correlation function decreases to half of its maximum value. The measurements which have been carried out with the Jicamarca radar facility yield a τ_ε of about 1.5 s for stratospheric heights. Since this coherence time is much larger than the pulse period of about 1 ms, it is possible coherently to add up M successive radar returns resulting from M radar pulses. This coherent integration procedure reduces the amount of data by a factor of M, where M has to be chosen such that $M \ \Delta t_p = \tau_c < \tau_\varepsilon$.

This coherent addition of M signals $\underline{s}(h_i, t_j)$ is equivalent to a digital filtering. To determine the transfer function of the digital filter system theory is used. The output signal resulting from the averaging process

$$\underline{S}'(h_i, t_n) = \frac{1}{M} \sum_{K=1}^{M} \underline{s}(h_i, t_n - k \cdot \Delta t_p) \tag{3}$$

can be interpreted as the result of the convolution of the input signal $\underline{s}(h_i, t_j)$ and the impulse response $h(t_j)$ of the filter. $h(t_j)$ itself is given by a finite "Dirac-comb":

$$h(t_j) = \sum_{K=1}^{M} \delta(t_j - k \cdot \Delta t_p) \ . \tag{4}$$

The transfer function $H(\omega)$ of the filter, which is given by the Fourier transform of the impulse response $h(t_j)$, has a shape of a comb filter. $|H(\omega)|$ is given by repeating the single sinc-functions

$$H_j(\omega) = 2 \cdot \Delta t_p \cdot \frac{\sin \omega M \Delta t_p}{\omega M \Delta t_p} \tag{5}$$

at intervals $1/\Delta t_p$. Each sinc-function has a half width of

$$\Delta f_{1/2} = \frac{1.8}{2\pi \cdot M \cdot \Delta t_p} \sim \frac{1}{M} \ , \tag{6}$$

which decreases with increasing number of averaged pulses.

The coherent integration or averaging procedure, which is performed in order to reduce the huge amount of data, acts as a low pass filter. In addition it also increases the signal-to-noise-ratio.

The amplification of the coherent signal is proportional to M, the number of additions, whereas the incoherent noise increases as $\sqrt{M}$. The resulting signal-to-noise amplitude ratio thereby increases as $\sqrt{M}$, and the signal-to-noise power ratio by a factor of M.

Figure 1 shows an example of plotted compressed data from measurements in the stratosphere. The pulse period used was 1 ms. With M = 288 the coherent integration time becomes 0.288 s, which is much less

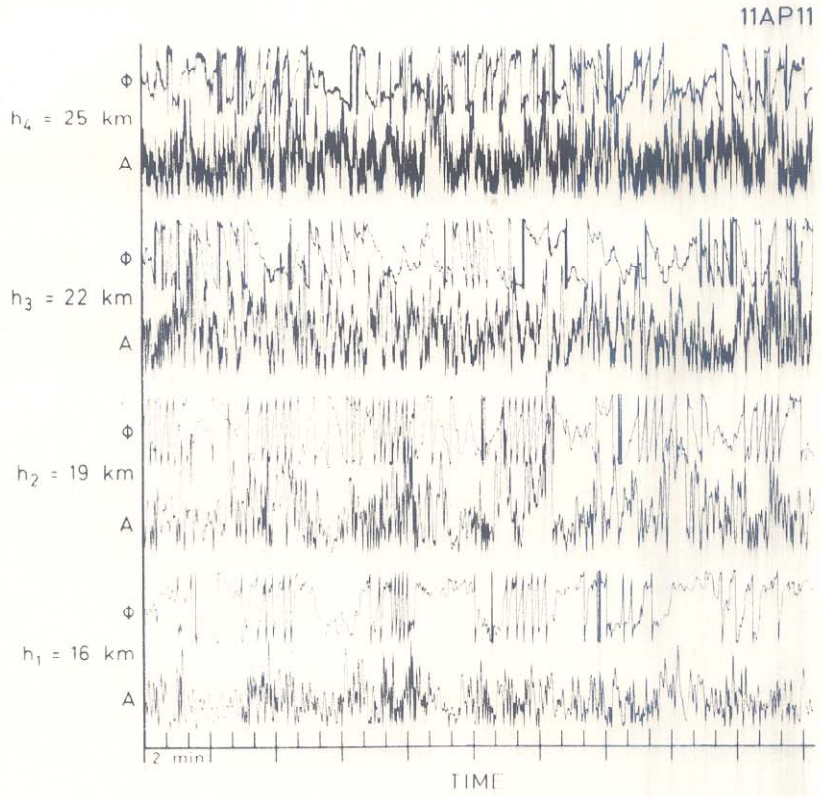

Fig. 1 Amplitude A and phase Φ (modul› 4π) of complex signals (raw data coherently integrated over 288 ms) backscattered from four stratospheric heights as a function of time.

than the signal correlation time τ_c of about 1.5 s. In Fig. 1 the amplitude A and the phase Φ (modulo 4π) of the complex signals for four different heights are plotted as a function of time. The high signal-to-noise ratio should be noted. Noise is equivalent to the width of the lines, which is first detectable at about 22 km. The amplitude A is related to the intensity of the backscattered signal, whereas the time derivative of the phase Φ is proportional to the line-of-sight velocity component of the scattering volume. This will be discussed further in section 2.3.

Before correlation methods can be used to deduce velocity and intensity information from the temporal and spatial variations of the signal, the constant parts superimposed on the signals have to be eliminated and the data have to be calibrated.

2.2 Calibration

The constant part of the signal caused by instrumental biases (DC) is eliminated by using the phase coding technique. The phase of the transmitted signal is changed by 180° from pulse to pulse. Simultaneously with the coherent integration procedure the corresponding decoding is performed so that the instrumental DC-part cancels. Further applications of coding are discussed by Kugel et al. (1978).

In addition to the instrumental biases the constant parts of the signal may arise from stationary radar targets such as mountains. Since this ground clutter can be very strong, so that the weaker temporal fluctuations of the signal are concealed, these constant parts are eliminated in the next step of the data-processing. The best estimate of the ground clutter $\underline{D}(h_i)$ is the average of the signal $\underline{S}'(h_i, t_n)$ for the total observational period T_o

$$\underline{D}(h_i) = \begin{pmatrix} D_R(h_i) \\ D_I(h_i) \end{pmatrix} = \begin{pmatrix} \langle S'_R(h_i, t_n) \rangle \\ \langle S'_I(h_i, t_n) \rangle \end{pmatrix} . \tag{7}$$

Subtracting these constant parts from the signal $\underline{S}'(h_i, t_n)$ yields

$$\hat{\underline{S}}(h_i, t_n) = \underline{S}'(h_i, t_n) - \underline{D}(h_i) . \tag{8}$$

The two components of this signal $\hat{S}_R(h_i, t_n)$ and $\hat{S}_I(h_i, t_n)$ should be statistically independent and their average intensities should be the same.

Usually, however, this is not the case because the quadrature detector shows phase errors and the two channels of the signal are differently amplified. A matrix $\mathbb{B}$, therefore, will be determined such that the signal $\hat{\underline{S}}$ is corrected and transformed into the signal $\underline{S}$ by

$$\underline{S} = \mathbb{B} \cdot \hat{\underline{S}} \tag{9}$$

where the components of $\underline{S}$ are statistically independent and the intensities of both are the same on average.

For this transformation the covariance matrices of $\underline{S}$ and $\hat{\underline{S}}$ are introduced:

$$\mathbb{R}(\hat{\underline{S}}) = \begin{pmatrix} \langle \hat{S}_R^2 \rangle & \langle \hat{S}_R \cdot \hat{S}_I \rangle \\ \langle \hat{S}_I \cdot \hat{S}_R \rangle & \langle \hat{S}_I^2 \rangle \end{pmatrix} \tag{10}$$

$$\mathbb{R}(\underline{S}) = \begin{pmatrix} \frac{\sigma^2}{2} & 0 \\ 0 & \frac{\sigma^2}{2} \end{pmatrix} \tag{11}$$

where σ^2 is given by the average power of the signal $\hat{\underline{S}}$, which has to be the same for the signal $\underline{S}$:

$$\sigma^2 = \langle \hat{S}_R^2 \rangle + \langle \hat{S}_I^2 \rangle = \langle S_R^2 \rangle + \langle S_I^2 \rangle . \tag{12}$$

Knowing $\mathbb{R}(\hat{\underline{S}})$, the transformation matrix $\mathbb{B}$ is determined such that the covariance matrix of $\underline{S}$ is equal to $\mathbb{R}(\underline{S})$.

The desired signal, therefore, has to satisfy the following equations:

$$\begin{aligned} \langle S_R^2 \rangle &= \frac{\sigma^2}{2} \\ \langle S_I^2 \rangle &= \frac{\sigma^2}{2} \\ \langle S_R \, S_I \rangle &= 0 \quad . \end{aligned} \tag{13}$$

From the point of view of matrix algebra this procedure is equivalent to the similarity transformation of the covariance matrix of $\hat{\underline{S}}$ to the covariance matrix of $\underline{S}$ by means of the transformation matrix $\mathbb{B}$

$$\mathbb{R}(\underline{S}) = \frac{\sigma^2}{2}\mathbb{E} = \mathbb{B}^{-1} \cdot \mathbb{R}(\hat{\underline{S}}) \cdot \mathbb{B} \quad . \tag{14}$$

$\mathbb{E}$ being the unit matrix.

Since it is known, that deterioration of the signal may result from phase errors of the quadrature detector and from different amplifications of the two channels of the signal, the transformation matrix $\mathbb{B}$ can be separated into amplitude and angle dependent parts. $\mathbb{B}$, therefore, can be expressed as the product of two more simple matrices:

$$\mathbb{B} = \mathbb{B}_A \cdot \mathbb{B}_W \tag{15a}$$

with

$$\mathbb{B}_A = \begin{pmatrix} a & o \\ o & b \end{pmatrix} \tag{15b}$$

and

$$\mathbb{B}_W = \begin{pmatrix} 1 & \sin\theta \\ 0 & \cos\theta \end{pmatrix} \quad . \tag{15c}$$

Geometrically the transformation with the matrix $\mathbb{B}$ can be interpreted as a rectification of an ellipse with oblique axes and a simultaneous mapping to a circle.

This calibration procedure leads ultimately to the determination of the three quantities a, b and θ. The solution of equation (9) allowing for (13) and (15) yields:

$$\theta = \arcsin - \frac{\hat{\sigma}^2_{RI}}{\hat{\sigma}^2_I} \tag{16a}$$

$$a^2 = \frac{\sigma^2/2}{\hat{\sigma}^2_R - (\hat{\sigma}^2_{RI} \cdot \hat{\sigma}^2_{RI})/\hat{\sigma}^2_I} \tag{16b}$$

$$b^2 = \frac{\sigma^2/2}{\hat{\sigma}^2_I - (\hat{\sigma}^2_{RI} \cdot \hat{\sigma}^2_{RI})/\hat{\sigma}^2_I} \tag{16c}$$

with $\quad \hat{\sigma}^2_R = \langle \hat{S}^2_R \rangle$

$$\hat{\sigma}^2_I = \langle \hat{S}^2_I \rangle$$

$$\hat{\sigma}^2_{RI} = \langle \hat{S}_R \cdot \hat{S}_I \rangle \quad .$$

2.3 Statistical analysis

At this stage methods of spectral analysis are applied to the compressed and corrected data in order to calculate the temporal and spatial variation of physical quantities like e.g. echo-power P, velocity v, turbulence-intensity ε. These quantities are deduced from the first three moments of the power spectrum $E(\omega)$ of the signal, or from the first three derivatives with respect to time of the autocorrelation

function $C(\tau)$, since $E(\omega)$ and $C(\tau)$ are Fourier transforms (FT) of each other. (A straight line should indicate a relationship.)

$$S(t) \overset{FT}{\Longleftrightarrow} F(\omega)$$

$$C(\tau) \overset{FT}{\Longleftrightarrow} E(\omega) = |F(\omega)|^2$$

$$P \longrightarrow \int E(\omega)\, d\omega \longrightarrow C(o)$$

$$v \longrightarrow \int \omega E(\omega)\, d\omega \longrightarrow C'(o)$$

$$\varepsilon \longrightarrow \int \omega^2 E(\omega)\, d\omega \longrightarrow C''(o)\ .$$

Figure 2 shows an example of a time sequence of amplitude spectra for 18 successive heights of radar-echoes, which have been recorded using the SOUSY-VHF-radar with a vertically pointing antenna beam.

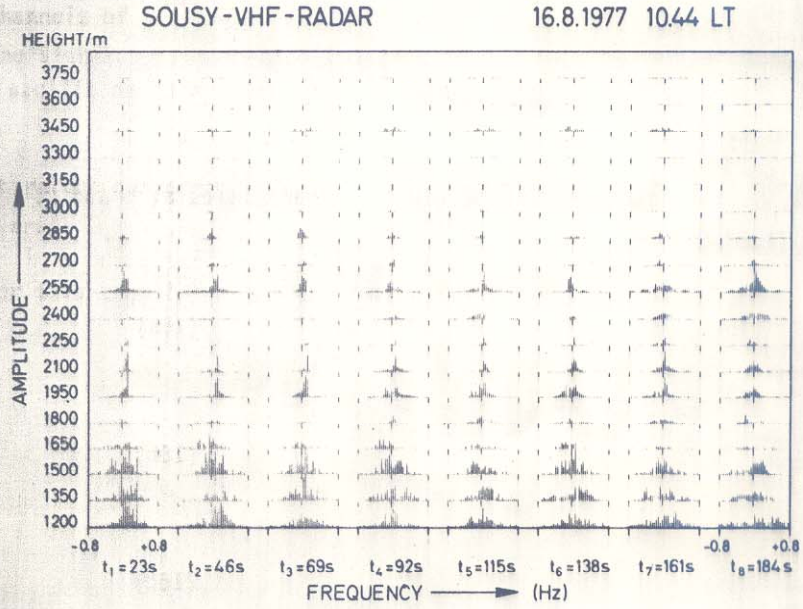

Fig. 2 Time sequence of amplitude spectra measured at 18 tropospheric heights for a frequency range of ± 0.8 Hz. Integration time 23 s (64 points), resolution 0.04 Hz.

The integration time T for calculating the spectrum, which has to be larger than the correlation time τ_ε, was 23 s. The figure shows the spatial and temporal variations of the echo-amplitude, which in turn are related to reflecting or backscattering layers. The maximum thickness of the layer is 150 m at a height of 3450 m and about 300 m at 1950 m. In addition the amplitudes for a fixed height sometimes show temporal variations within a time scale of 2 - 3 min.

The maximum frequency and the frequency resolution are given by

$$f_{max} = \frac{1}{2\, M\, \Delta t_p} = \frac{1}{2\, \tau_c} = 1.4 \text{ Hz}$$

$$f_{min} = \Delta f = \frac{1}{T} = 0.044 \text{ Hz}. \qquad (17)$$

The measured Doppler-shift is related to the mean background velocity, with which the reflecting or scattering layers move within the period T. Since the antenna beam was directed upwards, the radial velocity v_r reflects the vertical motion, which is of the order of a few tens of cm/s.

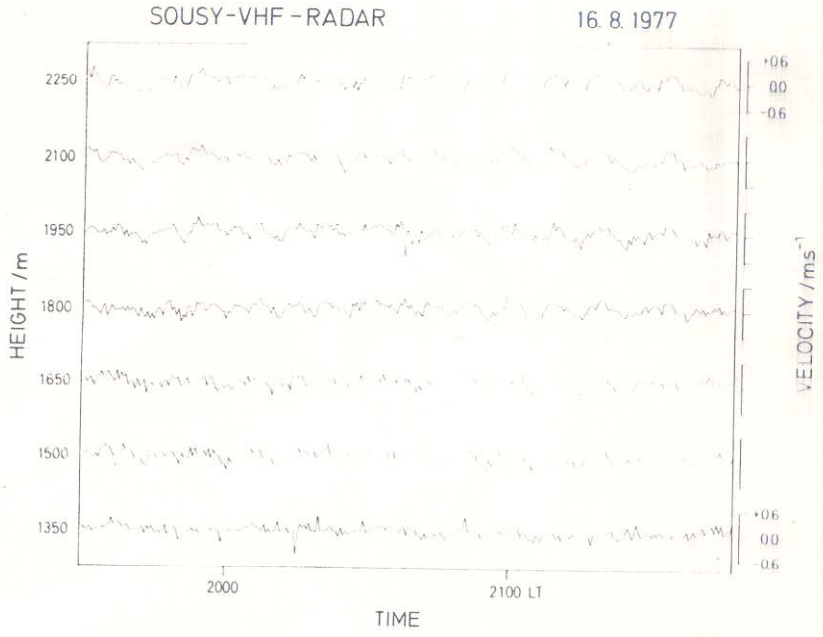

Fig. 3 Time series of the radial velocity for 7 tropospheric heights.

Figure 3 presents the variation of the radial velocity for a period of 2.5 hours for 7 successive heights measured with the SOUSY-VHF-radar. The integration time T was equal to 30 s. Apart from short-time variations, very stable oscillations with a period of about 9 minutes are observed in a height range from 1500 to 2250 m. Within the limits of accuracy the observed period of the velocity oscillations agrees quite well with the Brunt-Väisälä period for that height range. A more detailed investigation and a physical interpretation lies outside the scope of this paper and will be discussed and published separately (Rüster et al., 1977).

References

Aso, T.
Kato, S.
Harper, R.M.
1977
Arecibo middle atmosphere experiments
Geophys. Res. Letters 4, No. 1, 10-12

Balsley, B.B.
Cianos, N.
Farley, D.T.
Baron, M.J.
1977
Winds derived from radar measurements in the arctic troposphere and stratosphere
To be published.

Crane, R.K.
1970
Measurement of clear air turbulence in the lower stratosphere using the Millstone Hill L-band radar
14th Radar Meteor. Conf., Tucson, Ariz., Amer. Meteor. Soc., 101-106

Cunnold, D.M.
1975
Vertical Transport Coefficients in the Mesosphere Obtained from Radar Observations
J. Atmos. Sci. 32, 2191-2200

Czechowsky, P.
Klostermeyer, J.
Röttger, J.
Rüster, R.
Schmidt, G.
Woodman, R.F.
1976
The SOUSY-VHF-Radar for tropo-, strato- and mesospheric sounding
17th Radar Meteor. Conf., Seattle, Wash., Amer. Meteor. Soc., 349-353

Green, J.L.
Warnock, J.M.
Winkler, R.H.
VanZandt, T.E.
1975
A sensitive VHF radar for the study of winds, waves and turbulence in the troposphere, stratosphere and mesosphere.
16th Radar Meteor. Conf., Amer. Meteor. Soc., 313-315

Kugel, R.P.
Schmidt, G.
Woodman, R.F.
1978 Die Prozeßsteuerung und Datenerfassung der SOUSY-VHF-Radaranlage
Kleinheubacher Ber. 21

Rüster, R.
Woodman, R.F.
1976 Radar-Measurements in the Tropo-, Strato- and Mesosphere.
17th Radar Meteor. Conf., Seattle, Wash., Amer. Meteor. Soc. 354-358

Rüster, R.
Röttger, J.
Woodman, R.F.
1977 Radar Measurements of Waves in the Lower Stratosphere
To be published.

VanZandt, T.E.
Green, J.L.
Warnock, J.M.
Winkler, R.H.
1975 Studies of winds in the upper troposphere with a sensitive VHF-radar.
16th Radar Meteor. Conf., Amer. Meteor. Soc., 316-317

Woodman, R.F.
Guillen, A.
1974 Radar Observations of Winds and Turbulence in the Stratosphere and
Mesosphere.
J. Atmos. Sci. 31, 493-505